# Combined Action Potential- and Dynamic-Clamp for Accurate Computational Modeling of the Kinetics of Cardiac $I_{Kr}$ Current

Chiara Bartolucci[1], Claudia Altomare[2], Marco Bennati[1], Simone Furini[3], Antonio Zaza[2], Stefano Severi[1]

[1]University of Bologna, Cesena, Italy
[2]University of Milan Bicocca, Milan, Italy
[3]University of Siena, Siena, Italy

## Abstract

*The aims of this work were the optimization of the $I_{Kr}$ model, based on the Luo-Rudy (LRd) formulation by fitting it to $I_{Kr}$ recorded as E4031-sensitive current ($I_{E4031}$) under Action Potential clamp and the validation of the optimized model by testing its suitability to replace native $I_{Kr}$ under Dynamic Clamp conditions. We found the experimental $I_{E4031}$ very different from the $I_{Kr}$ based on the LRd model. We therefore looked for an $I_{Kr}$ formulation which better fit our experimental data. By solving a minimization problem we found an "optimized" formulation of the $I_{Kr}$ model. The optimized model was validated by using the dynamic clamp technique: we considered the AP traces in control conditions, under $I_{Kr}$ block, after injection of the modeled LRd $I_{Kr}$ and after injection of the optimized modeled $I_{Kr}$. Dynamic clamp experiments showed that the LRd $I_{Kr}$ shortens too much the action potential while our model brings back the AP closer the control AP morphology and duration.*

## 1. Introduction

Computational models of cardiac Action Potential (AP) are nowadays a very important tool to investigate the interaction between membrane ion channels with dynamically changing ionic concentrations and varying transmembrane voltage. These interactions are nonlinear, making the single cell a complex interactive system where a high degree of synthesis and integration occurs.

AP models are built by integrating the description of several individual membrane currents, which work in concert to induce both dramatic and subtle changes to the AP and to reproduce physiological and pathological conditions.

Ionic current models are largely based on traditional voltage clamp (V-clamp) experiments (carried out with non-physiological rectangular voltage pulses designed to study biophysical properties of the currents) and formulated with the Hodgkin-Huxley formalism. However, current models are seldom validated against current profiles experimentally measured during the AP.

Innovative experimental approaches are now available to assess 1) the dynamical behaviour of an individual currents during an imposed AP (AP-clamp technique, see e.g. [1]) and 2) the impact of modelled current features on freely changing AP (Dynamic Clamp, DC, [2]).

AP-clamp is a variation of V-clamp in which an AP waveform replaces the square wave pulse and an individual current is dissected from the total one by subtraction, as the current sensitive to a specific blocker.

Dynamic clamp is a real-time hybrid computational-biologic technique that has been recently developed to investigate the basic cellular mechanisms of AP formation, transfer and synchronization in health and disease. According to this technique a modeled current is injected into a myocyte while recording its effect on AP (current clamp mode). However, unlike classic current clamp, this current in not kwon *a priori*. The dynamic clamp technique operates in a continuous real-time loop, whereby membrane potential, recorded from the myocyte, is fed to a computer that calculates modeled current. The latter is injected back to the myocyte. The corresponding endogenous myocyte current can be pharmacologically blocked, thus being actually replaced by the modeled one. This provides an unique opportunity to test the AP response to specific current modifications, implemented in the model, in the context of a native myocyte.

The present work aims to 1) optimize an $I_{Kr}$ model by fitting it to $I_{Kr}$ recorded under AP-clamp; 2) validate the model by testing its suitability to replace native $I_{Kr}$ under dynamic clamp conditions.

This is particularly relevant given the essential role $I_{Kr}$ plays in repolarization and the consequent interest in evaluating the impact of its modifications on repolarization stability. At the macro level, the latter plays a pivotal role in arrhythmogenesis in general and in the genesis of "*torsades de pointes*" ventricular tachycardias in particular. The latter is an arrhythmia

commonly associated to prolongation of repolarization by drugs or genetic channel abnormalities (Long Q-T syndromes).

## 2. Methods

### 2.1. Action potential clamp

An action potential waveform (APW, averaged from 5 cycles) was recorded during steady-state pacing at a constant cycle length (CL) in control solution. After switching the same myocyte to V-clamp mode, the APW was applied, at the same CL, as command potential and control $I_m$ (virtually null, except for the stimulation artifact) was recorded. Challenge with the $I_{Kr}$ blocker E4031 (5 µM) elicited an inward current (compensation $I_m$), which was also recorded. The E4031-sensitive current ($I_{E4031}$, representative of $I_{Kr}$) was obtained by digitally subtracting compensation $I_m$ from control $I_m$. Extracellular bath solution included (in mM): 154 NaCl, 4 KCl, 2$CaCl_2$, 1 $MgCl_2$, 5 HEPES/NaOH e 5.5 D-Glucosio, a pH 7.35. Pipette intracellular solution contained (mM): 110 $K^+$-Aspartate, 23 KCl, 0.4 $CaCl_2$ ($Ca^{2+}$ free = $10^{-7}$ M), 3 $MgCl_2$, 5 HEPES KOH, 1 EGTA KOH, 0.4 GTP-Na salt, 5 ATP-Na salt, 5 creatine phosphate Na salt, pH 7.3.

### 2.2. $I_{Kr}$ model

We based the identification of $I_{Kr}$ model on the Luo-Rudy (LRd) formulation [3], which is until today the most widely used model of guinea pig ventricular AP. The formulation of $I_{Kr}$ incorporated both a time-dependent activation gate, $X_r$, and a time-independent inactivation gate, R, to approximate the very fast inactivation process of the HERG channels:

$$I_{Kr} = G_{Kr} * X_r * R * (V - E_{Kr}),$$

$$\frac{dXr}{dt} = \frac{Xr_\infty - Xr}{\tau_{Xr}}$$

$$E_{Kr} = -\frac{RT}{F} \ln \frac{[K]_o}{[K]_i},$$

where V is the membrane potential, $E_{Kr}$ is the reversal potential, and $G_{Kr}$ is the maximum conductance of $I_{Kr}$ According to the experimental conditions, we set

$$[K]_o = 4 \text{ mM}, [K]_i = 140 \text{ mM}.$$

The LRd model used the formulation of steady state activation, $Xr_\infty$, from [4] and formulated the voltage dependence of activation time constant, $\tau_{Xr}$, to fit their measurements (Fig. 1, black).

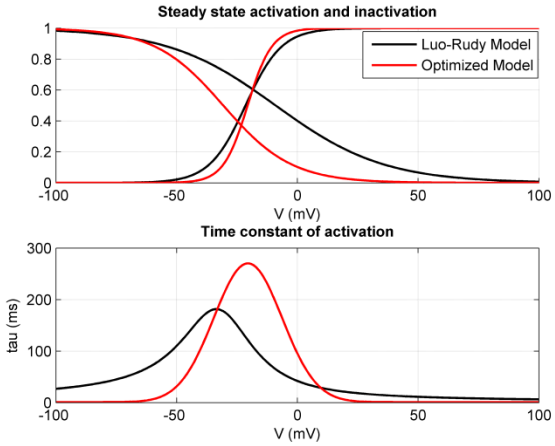


Figure 1. Steady state activation/inactivation (top) and time constant of activation (bottom) in the LRd model (black) and in the optimized model (red).

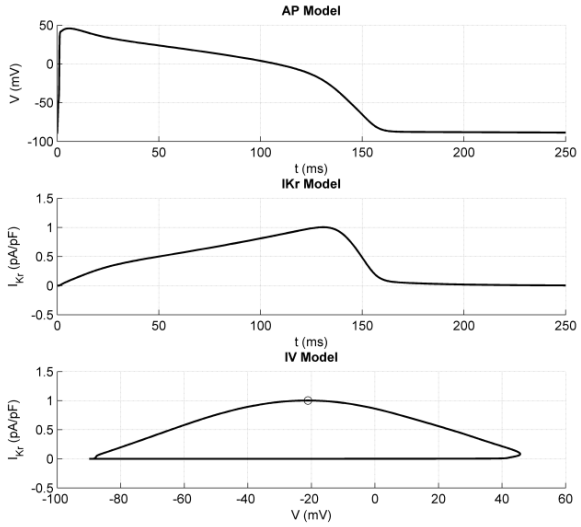


Figure 2. Action potential (top) and $I_{Kr}$ current (middle) generated from the LRd model; IV curve form the LRd model (bottom).

For the identification of the model parameters we minimized a cost function mainly based on least square difference between experimental and simulated $I_{Kr}$ time course during AP and that also weighted the difference between the experimental and simulated $V_{peak}$, that is the potential for which $I_{Kr}$ reach its maximal amplitude. We used also some constraints, based on our physiological knowledge, to restrict the parameter space.

### 2.3. Dynamic clamp

Dynamic clamp was used to simulate the presence of an additional conductance in the membrane of an isolated

myocyte. In this configuration, the membrane potential of the myocyte was continuously sampled into a personal computer, which calculated the voltage-dependent current and sent a command potential to the amplifier to inject the current into the myocyte (Fig. 3).

To implement the dynamic clamp we used an amplifier (Multiclamp 700B, Axon Instruments) connected to a data acquisition board (DAQ, 6024E PCI, National Instruments) on a personal computer (Intel Celeron 3.20GHz). The open source Real-Time Experiment Interface (RTXI [5]) was used: it is a fast and versatile real-time biological experimentation system based on Real-Time Linux. System features and custom user code were implemented as modules written in C++.

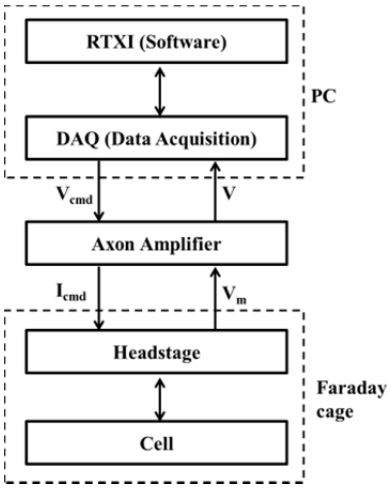


Figure 3. Block diagram of the system of dynamic clamp.

## 3. Results

### 3.1. Model identification: AP clamp

The AP clamp technique was used to obtain the drug (E4031) – sensitive current ($I_{E4031}$). The same experimentally recorded AP was used to compute $I_{Kr}$ with the LRd equation. As we can see from the example reported in Fig. 4 (middle and bottom) the $I_{E4031}$ current is very different from that of LRd model. In particular, the simulated current is larger during the plateau phase.

AP clamp data were then used to optimize the model leading to the following formulations of the steady state activation/inactivation and time constant activation:

$$Xr_{\infty} = \frac{1}{1 + e^{\frac{-(V-(-20.6))}{5}}}$$

$$\tau_{Xr} = 270 * e^{\frac{-(V-(-20.5))^2}{400}} + 1$$

$$R = \frac{1}{1 + e^{\frac{V-(-30.7)}{14}}}$$

which are also shown in Fig. 1 (red trace), compared to the original LRd formulation.

As shown in Fig. 4 and Table 1 the optimized model allowed a satisfactory reproduction of experimental $I_{E4031}$ features.

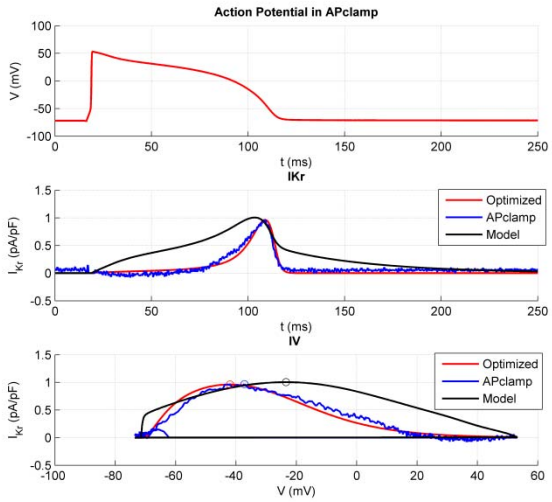


Figure 4. Example of experimental AP used in the AP clamp technique (top) to measure the corresponding E4031–sensitive current (blue) and to compute offline the $I_{Kr}$ current with the LRd model (black) and with the optimized model (red) (middle). IV curve of the $E_{4031}$–sensitive current (blue), of the $I_{Kr}$ current with the Luo-Rudy model (black) and with the optimized model (red) (bottom).

Table 1. Properties of $I_{Kr}$: experimental, LRd model and optimized model

| | Exp | LRd Model | Optimized Model |
|---|---|---|---|
| $V_{peak}$ (mV) | -46 ± 7.5 | -21.09 | -40.8991 |
| $I_{peak}$ (pA/pF) | 0.86 ± 0.28 | 1.00 | 0.94 |
| $I_{mean}$ (pA/pF) | 0.17 ± 0.16 | 0.59 | 0.24 |
| TTP (ms) | 153 ± 77 | 125 | 135 |
| TTP(%) | 95± 2 | 82 | 88 |
| $I_{mean}$ plateau | 0.1± 0.1 | 0.4947 | 0.1 |

A comprehensive comparison between AP clamp experiments and simulated AP clamp was reported in Table 1. It shows: the peak of the AP in corresponding to the peak of the current, $V_{peak}$; the peak of the current, $I_{peak}$; the mean of the current during the AP, $I_{mean}$; the difference between the time corresponding to the peak current and the time of the AP maximum, TTP (time to

peak); TTP % obtained as the ratio between TTP and $ADP_{90}$, times 100; the mean of current during the plateau, $I_{mean}$ plateau. We consider the plateau duration as the period between the AP maximum and the instant of time when the AP first derivative becomes greater than -1.

### 3.2. Model validation: dynamic clamp

After identification the $I_{Kr}$ model was tested in a protocol where the AP was recorded in control condition and after AP prolongation induced by $I_{Kr}$ block with $E_{4031}$. After that, we injected both the formulation of the current: LRd and optimized. An example of the results of this loop is shown in Fig. 6 where we reported the 4 AP traces (in control, under $I_{Kr}$ block, after the injection of LRd and optimized model). In the bottom panel we see the different injected currents, LRd and optimized.

A preliminary quantitative comparison was performed by computing several AP features in 4 cells. We consider the $APD_{90}$, $APD_{50}$, $APD_{30}$, calculated as the AP duration starting from the AP maximum until the 90%, 50% and 30% of repolarization; the PD (plateau duration) and the VRepMax (maximum velocity repolarization) calculated as the maximum of the AP first derivative.

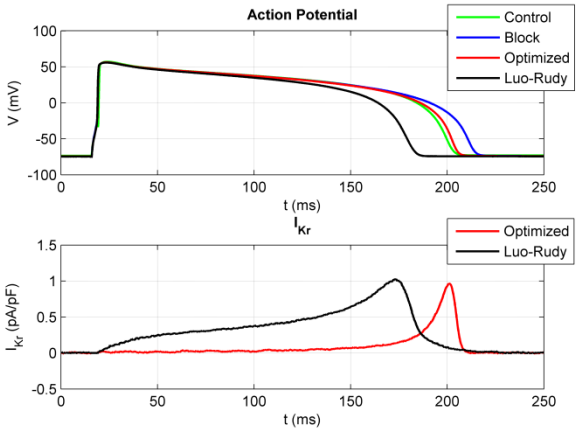


Figure 5. Example of dynamic clamp experiment.

Table 2. Characteristics of AP during the dynamic clamp experiments.

| | CTR | $I_{Kr}$ Block | LRd | Opt |
|---|---|---|---|---|
| $APD_{90}$ (ms) | 139 | 152 | 121 | 143 |
| $APD_{50}$ (ms) | 124 | 134 | 107 | 128 |
| $APD_{30}$ (ms) | 100 | 105 | 88 | 103 |
| PD (ms) | 87 | 95 | 74 | 90 |
| VrepMax (mV) | -49 | -51 | -49 | -49 |

## 4. Conclusion

AP clamp data pointed out significant differences between experimentally measured $I_{E4031}$ profile and the time course predicted by the LRd $I_{Kr}$ model. The $I_{Kr}$ model was then successfully optimized by fitting it to $I_{Kr}$ recorded under AP-clamp. The main changes in the optimized model with respect to the original one are a more pronounced inactivation at negative potential and a positive shift of the voltage dependence of activation time constant (Fig. 1). Consistency of this result with the large, and variable, amount of V-clamp experimental data reported in literature deserves a detailed analysis.

A preliminary validation of the model was performed by testing its suitability to replace native $I_{Kr}$ under dynamic clamp conditions and restore the baseline AP features, in particular AP duration, whereas the excessive amount of repolarizing current computed by the LRd model during the plateau phase led to over reduction of AP duration (Fig. 6).

The optimized model could be used to explore the effects of changes in single kinetic parameters on the AP and to study pathologies linked with $I_{Kr}$ alterations.

## References


[1] Rocchetti M, Besana A, Gurrola GB, Possani LD, Zaza A. Rate dependency of delayed rectifier currents during the guinea-pig ventricular action potential. J Physiol 2001; 534: 721–732.

[2] Wilders R. Dynamic clamp: a powerful tool in cardiac electrophysiology. J Physiol 2006; 576.2: 349-359.

[3] Zeng J, Laurita KR, Rosenbaum DS, Rudy Y. Two components of the delayed rectifier $K^+$ current in ventricular myocytes of the guinea pig type. Circulation Research 1995;77:140-152.

[4] Sanguinetti MC, Jurkiewicz NK. Two components of cardiac delayed rectifier $K^+$ current: differential sensitivity to block by class III antiarrhythmic agents. J Gen Physiol 1990;96:195-215.

[5] http:// www.rtxi.org.



Address for correspondence.

Stefano Severi
DEI, University of Bologna, Cesena,
Via Venezia 52, 47521, Cesena (FC), Italy
stefano.severi@unibo.it